

High-resolving electrostatic energy analyzer with fine tuning for space investigations

I.A.Ilyina and A.M.Ilyin*

National Nanolaboratory, Kazakh National University, Almaty, Kazakhstan

Abstract: The paper presents results of numerical calculations of a high-resolving electrostatic energy analyzer, based on a bounded cylindrical field, for investigations of flows of charged particles in space. The analyzer possesses with ability of fine tuning of focusing characteristics, using an additional tuning potential, applied to one of electrodes. A combination of high energy resolution ability with high transmission, simple design and compactness makes this instrument very promising for space technologies.

I. INTRODUCTION

There are many applications, especially in space charged particles flows studies, in which electrons or protons originating from distant objects (for example, solar wind) move in space as nearly parallel flows. Therefore, electrostatic energy analyzers combining high electron-optical characteristics with a compact and simple design are needed. Analyzers with toroidal or spherical electrodes [1,2] are well known for a long time, but these instruments have a complicated shape of electrodes and need special systems for fringe-field correction. In the recent paper [3] it was shown that a well known cylindrical mirror field [4] provides only first-order focusing for a flow of charged particles entering directly between electrodes parallel to axis of symmetry and also requires a fringe-field correction system. In the paper [5] it was found out, that that a cylindrical field bounded along axis of symmetry can prove the second order focusing for a parallel flow of charged particles. In the present paper we consider results of the theoretical investigations of the focusing properties of a bounded cylindrical field, in order to build a high energy resolving, compact and free of fringe-field distortion effects energy analyzer for measurements of energetic characteristics of charged particle flows. For example, such instrument can find out application in measurements of solar wind flows and for forecasting the rapid changes of solar activity.

II. CALCULATIONS

The electrostatic field that has been used is a solution of the Laplace equation

$$\Delta U(R, Z) = 0 \quad (1)$$

with boundary conditions

$$U(R_1, Z) = U(R, 0) = 0, U(R_2, Z) = U_0, U(R, L) = V$$

The field is restricted by concentric cylindrical surfaces with radii R_1 and R_2 and two flat surfaces perpendicular to the z -axis [6] with a distance L between them (see figure 1). The potential distribution of this electrostatic system can be written in Appendix.

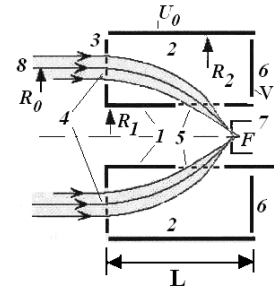


Fig 1. The schematic cross-section view of the analyzer developed. 1- the inner cylindrical electrode (with zero-potential), 2- the outer cylindrical electrode with a bending potential U_0 , 3- a first face plate with the entrance window 4, 5 - the exit window made in the inner electrode, 6- the second plate, isolated of other electrodes, to which a tuning potential V is applied. 7 – a diaphragm of a detector, 8 – the flow of charged particles, entering the analyzer with R_0 – radial coordinate of the central trajectory, F – the focus point.

All lengths in (2) and below are scaled with a radius of the inner cylinder R_1 in order to introduce the dimensionless parameters: $r = R / R_1$, $z = Z / R_1$,

$$l = L / R_1, r_0 = R_0 / R_1, \beta = R_2 / R_1. \text{ Here,}$$

$$F_n(r) = [I_0(k_n r) \cdot K_0(k_n) - I_0(k_n) \cdot K_0(k_n r)] / K_0(k_n)$$

$$k_n = (2n + 1) \cdot \pi / l$$

I_0 and K_0 in (2) are modified Bessel and Hankel functions, respectively.

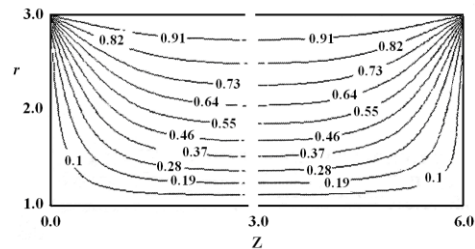


Fig 2. A typical map of a cross-section view of equipotential levels of the field formed with $V=0.04U_0$.

The map in the figure 2 was for simplicity build with $U_0 = 1$ and with the tuning potential $V = 0.04$. One can see obvious asymmetry in distribution of equipotential levels due to effect of small tuning potential on the right-side boundary. In order to shorten the picture the map is shown with a cut in the central part, where potential

levels are stationary. The non-relativistic equations of motions in the field (2) are given by

$$\ddot{r} = -\frac{e}{m} \frac{\partial U(r, z)}{\partial r}$$

(3)

$$\ddot{z} = -\frac{e}{m} \frac{\partial U(r, z)}{\partial z}$$

The system of differential Equations (3) has been numerically integrated to determine the individual trajectories of charged particles, entering the focusing field within the flow parallel to the axis of symmetry. Calculations were performed by the Runge-Kutta method with the absolute accuracy of the final coordinate about 0.0003. All details of the calculation were similar to given in papers [7-9]. Calculations have been made for a set of geometrical parameter β ranging from 2 to near 4, and the length of the analyzer l used was equal to 6. The second-order focusing regimes have been found for different sets of β and dimensionless energy coefficient $G = E_0 / eU_0$ (with E_0 —initial kinetic energy of a particle and U_0 —focusing potential, applied to the outer cylinder). The set of typical aberration figures numerically calculated is presented in figure 3. All curves have the shape of a cubic curve with a central inflection point, indicating the sharp second-order focusing [8]. We found that the value of G is relatively large for small β values and rapidly decreases for larger β within the second-order focusing mode. A high value of G is suitable for measurements of charged particles flows with larger energies, because they can be controlled by a low focusing potential.

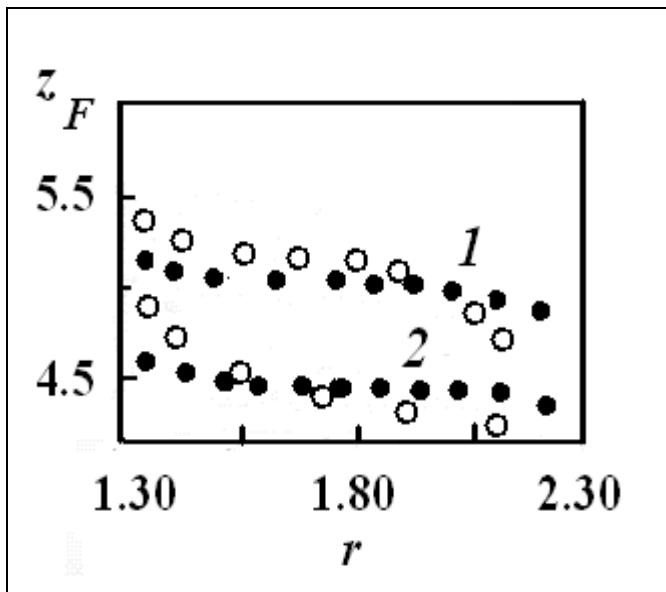
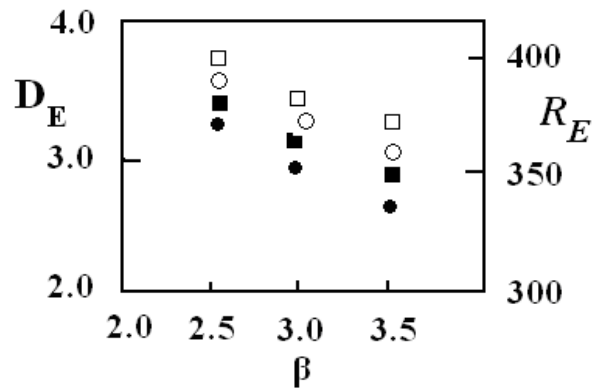
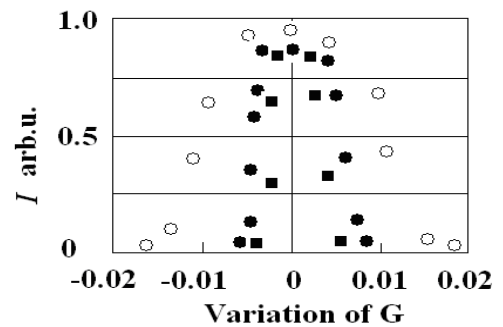


Fig 3. Typical aberration figures for different sets (β, G, V) illustrating the second order focusing regimes (all curves shaped like cubic parabola) and tuning effect. 1- (2.52, 2.6); 2- (3.0, 1.9); Light marks – $V=0$, black marks – $V = 0.04U_0$.

In our recent work [8] it was theoretically obtained for the case $V = 0$, that the interval of entering radial coordinates r within the second order focusing regime increases with β growing up. Data presented in figure 3 show, that using a small tuning potential V allows essentially enlarge entrance window with better focusing characteristics. In other words, tuning potential provides higher sensitivity with keeping very high resolution ability on energy.



(a)



(b)

Fig 4. a) Calculated dependence of energy dispersion D_E (black marks) and energy resolution ability R_E (light marks) on β for the second-order focusing mode; The circles – regimes with $V=0$, squares – regimes with $V = 0.04 U_0$. Obviously, both D_E and R_E can be noticeably modified by using tuning effect. b): The energy transmission function calculated for different configurations: 1) $\beta = 2.51, G_0 = 2.64$ and 2) $\beta = 3.0, G_0 = 1.96$.

Figure 4a presents the results of numerical calculations energy dispersion D_E and energy resolution ability R_E with β ranging from 2 to 4. For comparison, the calculation for a typical configuration of well known cylindrical mirror performed in the same way of estimation gave the value of about 290 that is in a good agreement with well known data [4]. Figure 4b shows the energy transmission functions for two sets of geometrical parameters with $V = 0$. One also can see the noticeable modification in the shape of transmission function by applying the small tuning potential

III. CONCLUSION

The focusing characteristics of the cylindrical face-field analyzer for a parallel flow of charged particles were numerically studied. Energy dispersion and energy resolution ability were calculated for a wide range of geometrical parameters and the shape of the energy function was determined. Sets of parameters which provide the sharp second-order focusing with high sensitivity were found out for several configurations. The instrument has very important feature for space applications: its focusing characteristics can be tuned finely by variation of small tuning potential applied to one of electrodes. The instrument in practical realization is very compact, has very simple design and does not require any fringe-field correction system that is very important for space applications.

REFERENCES

- [1] Decreau, P, Prange, R. and Berthelier, J.J. (1975) Optimization of Toroidal Electrostatic Analyzers for Measurements of Low Energy Particles in Space. *Rev.Sci.Instrum.* 46, 995-1007.<http://dx.doi.org/+10.1063/1.1134412>.
- [2] Purcell, E.M. (1938) The Focusing of Charged Particles by a Spherical Condenser. *Phys.Rev.* 54, 818-823.
- [3] Ilyin, A.M. (2000) About Some Focusing Properties of a Cylindrical Field. *J. Electron Spectrosc. Related Phenom.* 113, 1-4. Doi: 10.1016/S0368-2048(00)00176-6.
- [4] Risley, J.S. (1975) Design Parameters for the Cylindrical Mirror Energy Analyzer. *Rev.Sci.Instrum.* 43, 95-100.[doi: 10.1063/1.1685454](http://dx.doi.org/10.1063/1.1685454).
- [5] Ilyin, A.M. (2001) Focusing Properties of a Bounded Cylindrical Field. *J. Electron Spectrosc. Related Phenom.* 120, 89-92.[doi: 10.1016/S0368-2048\(01\)00308-5](http://dx.doi.org/10.1016/S0368-2048(01)00308-5).
- [6] Ilyin, A.M. and Borisov, B.A. (2001) Second-Order Focusing of a Bounded Cylindrical Field for a Distant Source. *Meas.Sci.Technol.* 12, 2015-2019. [doi:10.1088/0957-0233/12/11/335](http://dx.doi.org/10.1088/0957-0233/12/11/335).
- [7] Ilyin, A.M. 2003 New Class of Electrostatic Energy Analyzers with a Cylindrical Face-Field. *Nucl.Instrum.Methods Phys.Res. A* 500, 62-66. [doi:10.1016/S0168-9002\(03\)00334-6](http://dx.doi.org/10.1016/S0168-9002(03)00334-6).
- [8] A.M.Ilyin and I.A.Ilyina, .New electrostatic energy analyzer for space plasma measurements, *Journal of Instrumentation, JINST.* 2 (2007) P01002, [doi: 10.1088/1748-0221/2/01/P01002](http://dx.doi.org/10.1088/1748-0221/2/01/P01002).

APPENDIX

$$U(r, z) = \frac{4 \cdot U_0}{\pi} \cdot \sum_{n=0}^{\infty} \sin(2n+1) \frac{\pi \cdot z}{l} \frac{F_n(r)}{F_n(\beta) \cdot (2n+1)} + \frac{4 \cdot V}{\pi} \cdot \sum_{n=0}^{\infty} \sin((2n+1) \frac{\pi \cdot (r-1)}{\beta-1}) \cdot \frac{I_0((2n+1) \cdot \pi \cdot z / \beta)}{(2n+1) I_0((2n+1) \cdot \pi \cdot l / \beta)} \quad (2)$$